Identification, structure–activity relationships and molecular modeling of potent triamine and piperazine opioid ligands

Austin B. Yongye [a], Jon R. Appel [b], Marc A. Giulianotti [a], Colette T. Dooley [a], Jose L. Medina-Franco [a], Adel Nefzi [b], Richard A. Houghten [a,b], Karina Martínez-Mayorga [a,*]

[a] Torrey Pines Institute for Molecular Studies, 11350 SW Village Parkway, Room 132, Port St. Lucie, FL 34987, USA
[b] Torrey Pines Institute for Molecular Studies, 3550 General Atomics Court, San Diego, CA 92121, USA

ARTICLE INFO

ABSTRACT

Opioid receptors are important targets for pain management. Here, we report the synthesis and biological evaluation of three positional scanning combinatorial libraries, consisting of linear triamines and piperazines. A highly potent (14 nM) and selective ($IC_{50(\mu)}/IC_{50(\kappa)} = 71$; $IC_{50(\delta)}/IC_{50(\kappa)} = 714$) triamine for the κ-opioid receptor was found. In addition, non-selective μ–κ binders were obtained, with binding affinities of 54 nM and 22 nM for μ- and κ-opioid receptors, respectively. Structure–activity relationships of each subset are described. 3D molecular alignments based on shape similarity to internal and external query molecules were carried out. For the combinatorial chemistry dataset studied here a 1.3 similarity cut-off value was observed to be efficient in the ROCS-based alignment method. Interactions from the overlays analyzed in the binding sites of homology models of the receptors revealed specific substitution patterns for enhancing binding affinity in the piperazine series. Pharmacophore modeling of the compounds found from the three combinatorial libraries was also performed. The pharmacophore model indicated that the important feature for receptor binding activity with the μ-receptor was the presence of at least one hydrogen bond acceptor and one aromatic hydrophobic group. Whereas for the κ-receptor two binding modes emerged with one set of compounds employing the hydrogen bond acceptor and aromatic hydrophobic group, and a second set possibly via interactions with the receptor by hydrophobic and ionic salt-bridges.

© 2009 Elsevier Ltd. All rights reserved.

1. Introduction

The three opioid receptors μ, κ, and δ mediate analgesia; however, the types of pain inhibited, as well as their secondary functions, have been shown to differ. The μ-receptor has generally been regarded as the receptor primarily associated with pain relief[1] as well as tolerance and physical dependence.[2] The δ-receptor is associated with thermal analgesia,[1,3] but is also involved in respiratory depression[4] and addiction.[5,6] The κ-receptor is the most influential in affecting analgesia in response to pain induced by chemical stimuli,[7,8] but has also been shown to induce diuresis[9] and sedation.[10,11] Such differences in receptor function encourage the search for compounds that produce analgesia without the deleterious side effects of morphine or other opiate analgesics. Analogs of the natural opioid peptides have been used in drug discovery efforts to understand the intricacies of the opioid receptor family. More recently, highly selective compounds have been identified and used as research tools.[12,13] Nonetheless, the need for additional opiate receptor specific ligands remains. New ligands that differ in structure may prove to have improved pharmacology, for example, improvements in efficacy, in vivo half lives, and bioavailability.

The solid phase synthesis of mixture-based combinatorial libraries,[14] when combined with high throughput screening assays, represent a powerful approach for the discovery and generation of active receptor ligands. Moreover, mixture-based libraries arranged in a positional scanning format, provide extensive structure–activity information in any given assay. This is inherent with this approach as positional scanning libraries are composed of systematically arranged mixtures having defined and mixture positions. Thus, information regarding the activity of each functionality is obtained for each position of the library. Computational methodologies, alongside experimental data, provide critical insights for the understanding of structure activity relationships, binding mode prediction, and conformational stability, among others. Binding models developed to describe agonist and antagonist ligands have shown common as well as distinct pharmacophoric regions.[15] In addition, different binding modes have been proposed for structurally different molecules or even for the same molecule.[16] It is worth noting that the analysis presented in this work is based on binding affinity measurements. The homogeneous

* Corresponding author. Tel.: +1 772 345 4688; fax: +1 772 345 3649.
 E-mail address: kmartinez@tpims.org (K. Martínez-Mayorga).

SAR[17] observed in these molecular sets might be either an indicative of the same behavior (agonist vs antagonist) or represent common pharmacophoric regions to agonist and antagonist. In both cases, it is important to have the same binding mode and absence of activity cliffs.[18] As will be described, some molecules that do not follow the proposed models were observed. We report here the preparation of one triamine and two piperazine positional scanning libraries and their screening against the three opioid receptors. The solid phase synthesis of piperazine derivatives from resin-bound acylated dipeptides was previously described.[19] Following deconvolution of each library, novel triamines and piperazines with good affinity and selectivity for the κ-opioid receptor were identified, as well as good binders for the μ-opioid receptor with modest selectivity. Structure–activity relationships (SAR) are discussed. A binding model for selected active compounds is proposed based on similarity-based molecular alignment and pharmacophore modeling.

2. Results and discussion

2.1. Biological evaluation

The N-methylated 1,3,4-trisubstituted piperazine (TPI 760), N-benzylated 1,3,4-trisubstituted piperazine (TPI 761), and N-methyl triamine (TPI 762) libraries were screened against the μ, κ, and δ-opioid receptors. A total of 84 compounds was selected from the library screening results and synthesized for testing against the three opioid receptors. All assays contain a standard curve on every plate using standard mu, delta or kappa ligands and IC_{50}s are routinely determined. Overall, the 84 compounds derived from these libraries had good activity in the μ and κ-receptors, but little activity in the δ-receptor, Table 1. The N-methyl triamines were clearly more active in the κ-receptor than in the μ-receptor, and the N-methyl piperazines were more active than the N-benzylated piperazines for both μ and κ receptors. From the 84 compounds tested a subset of 43 compounds (Table 1) was further selected to propose a binding mode with the opioid receptors based on molecular alignment and pharmacophore modeling.

2.2. Structure–activity relationships

To describe the structure–activity relationship, the compounds were classified into 14 sets, as shown in Table 1. Compounds from library TPI 762 were partitioned into four sets (A–D) depending on whether the R1 and R2 substituents were aromatic or aliphatic. The activities of the compounds in sets A, B and C suggested that the nature of the cyclic group at R3 might play a role in binding. In set A, for example, with reference to the μ-receptor, changing R3 from a cycloheptyl (1: IC_{50} = 54 nM) to 4-methyl-1-cyclohexyl group (2: IC_{50} = 313 nM) decreased the activity by approximately sixfold. The substitution in the R3 position of cycloheptyl (1: IC_{50} 54 nM) to norbornylmethyl (4: IC_{50} 270 nM) resulted in a fivefold decrease, while the cyclopentylmethyl substituent (5: IC_{50} = 170 nM) reduced binding affinity by only threefold. It has been noted that for SAR data, a modification that results in at least a fivefold change in activity is considered significant.[20] A similar trend was observed with the κ-receptor, wherein the cycloheptyl to 4-methyl-1-cyclohexyl, norbornylmethyl and cyclopentylmethyl substitutions resulted in a four-, twenty- and eightfold decrease in activity, respectively. In contrast, most of the compounds in set D were inactive regardless of the group at the R3 position, except compound 20 (IC_{50} = 102 nM) that was active only with the κ-receptor.

In general, compounds in set B (R1: aromatic; R2: aliphatic) were more active with the κ-receptor than the μ-receptor, while the reverse was true for compounds in set C (R1: aliphatic; R2: aro-

matic). Compounds in set D had only aliphatic groups at R1 and R2 and were generally inactive, except compound 20, vide supra. Therefore, based on the activities of the compounds in sets A, B and C and the lack thereof for all the compounds in set D, the aromatic groups appears to play a role in binding for both receptors.
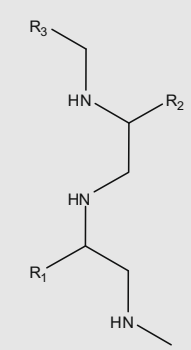
Between sets A and B, the overall trend was a reduction in activity to the μ-receptor when the R1 group was aromatic and the R2 group was aliphatic, whereas the same substitution resulted in an increase in activity toward the κ-receptor. Comparing the activities of set A with those of set C revealed an overall preference for the S-4-hydroxybenzyl group at R1 to the κ-receptor. Sets A and C were all active with the μ-receptor, albeit clear trends could not be established. The substitution patterns suggested that when R1 and R2 were both aromatic groups (set A), these compounds were active with both the μ- and κ-receptors. Aromatic and aliphatic groups at R1 and R2, respectively, (set B) tended to yield κ-selective ligands. On the other hand, an aliphatic group at R1 and an aromatic group at R2 generally resulted in modest μ-selective ligands, set C.
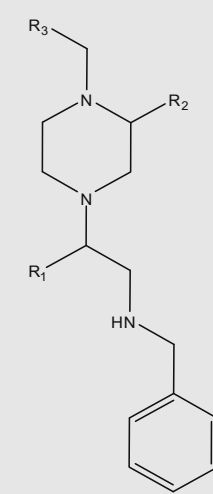
All compounds in this study derived from library 761 were inactive to the μ-receptor, while only compounds 46, 54 and 56 were active to the κ-opioid receptor. A possible explanation of the inactivity of these compounds is discussed below.

The N-methyl piperazines (TPI 762) were classified as shown in Table 1, based on differences of their R3 substituents. In addition, sets I and J, and sets K and L differed at their R2 substituents. Sets M and N varied at their R1 substituents, for example, compounds (73, 79) and (75, 81), while sets (J, L) and (I, K) differed in the stereochemistry of their R1 substituents. When the R2 substituent was a hydrogen atom all the compounds were active with both receptors regardless of the stereochemistry of the R1 substituents and the R3 group, with the exception of compound 66 that was inactive with the κ-receptor. Among this class of compounds (R2 = hydrogen) 66 was the only compound whose R3 substituent was neither aromatic nor cyclic. It was also the weakest binder for the μ-receptor among the actives. Set L could be generated from set K by substituting the hydrogen atom at the R2 position with an S-isopropyl group. The activity trends suggested that the presence of a more bulky isopropyl group at R2 would decrease the activity of the compounds in set L relative to set K. The general preference of a less bulky R2 substituent was also manifested, though to a lesser extent, when 60 and 64 were compared. It was also observed that the combination of an R-hydroxybenzyl group at R1 with S-stereochemistry at R2 resulted in compounds that were inactive with both receptors, evident in the activity profiles of the compounds in set L (69–72). The S-hydroxybenzyl group at R1 with S-stereochemistry at R2 showed better activity, manifested in sets J and L. Sets J and L also varied in the stereochemistry of the R1 position, with the compounds in sets J and L bearing the S- and R-stereochemistries, respectively. Switching the R1 stereochemistry of two μ-active compounds, 61 (206 nM) and 64 (223 nM) in set J, to generate compounds 69 (1000 nM) and 72 (1000 nM) in set L, respectively, led to a loss of activity. The affinities for the κ-receptor also exhibited a similar trend, except for compound 61 that was inactive in both scenarios.

Sets (I, K) could be differentiated by the stereochemistry of the R1 position: S-stereochemistry in set I and R-stereochemistry in set K. There was a slight preference for the R-stereochemistry for compounds in set K for the μ-receptor. Compounds in sets M and N were generally inactive against the μ-receptor, except compound 81 (336 nM). For the κ-receptor, in addition to compound 81 (230 nM), compounds 73 (58 nM) and 74 (119 nM) were both active. Interestingly, compounds 73 and 74 did not possess any aromatic groups, reminiscent of compound 20 from library 762, yet were active only with the κ-receptor.
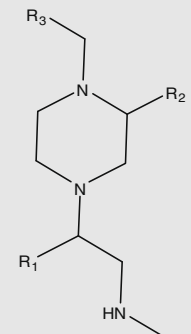
Table 1
Molecules identified as potential hits to opioid receptors from three different positional scanning libraries

Set	Molecule	Receptor[a]	R1	R2	R3	μIC$_{50}$ (nM)	κIC$_{50}$ (nM)	δIC$_{50}$ (nM)	pIC$_{50}$ μ	pIC$_{50}$ κ	Scaffold
A	1	Kappa	S-4-Hydroxybenzyl	S-4-Hydroxybenzyl	Cycloheptyl	54	22	>10,000[b]	7.27	7.65	
	2	Kappa	S-4-Hydroxybenzyl	S-4-Hydroxybenzyl	4-Methyl-1-cyclohexyl	313	102	>10,000	6.50	6.99	
	4	Kappa	S-4-Hydroxybenzyl	S-4-Hydroxybenzyl	Norbornylmethyl	270	452	>10,000	6.57	6.34	
	5	Kappa	S-4-Hydroxybenzyl	S-4-Hydroxybenzyl	Cyclopentylmethyl	170	186	2878	6.77	6.73	
B	6	Kappa	S-4-Hydroxybenzyl	R-Propyl	Cyclopentylmethyl	648	97	>10,000	6.19	7.01	
	7	Kappa	S-4-Hydroxybenzyl	R-Propyl	4-Methyl-1-cyclohexyl	>1000	14	>10,000	6.00	7.85	
	8	Kappa	S-4-Hydroxybenzyl	R-Propyl	Adamantylmethyl	530	37	>10,000	6.28	7.43	
	9	Kappa	S-4-Hydroxybenzyl	R-Propyl	Norbornylmethyl	174	17	2104	6.76	7.77	
	10	Kappa	S-4-Hydroxybenzyl	R-Propyl	Cycloheptyl	238	25	2749	6.62	7.60	
C	11	Kappa	R-Propyl	S-4-Hydroxybenzyl	Cycloheptyl	107	439	>10,000	6.97	6.36	
	12	Kappa	R-Propyl	S-4-Hydroxybenzyl	4-Methyl-1-cyclohexyl	225	1747	>10,000	6.65	5.76	
	14	Kappa	R-Propyl	S-4-Hydroxybenzyl	Norbornylmethyl	178	333	>10,000	6.75	6.48	
	15	Kappa	R-Propyl	S-4-Hydroxybenzyl	Cyclopentylmethyl	240	766	>10,000	6.62	6.12	
D	16	Kappa	R-Propyl	R-Propyl	Cycloheptyl	>1000[b]	>1000	>10,000	6.00	6.00	
	17	Kappa	R-Propyl	R-Propyl	4-Methyl-1-cyclohexyl	>1000	>1000	>10,000	6.00	6.00	
	18	Kappa	R-Propyl	R-Propyl	Adamantylmethyl	>1000	>1000	>10,000	6.00	6.00	
	19	Kappa	R-Propyl	R-Propyl	Norbornylmethyl	>1000	>1000	>10,000	6.00	6.00	
	20	Kappa	R-Propyl	R-Propyl	Cyclopentylmethyl	>1000	102	>10,000	6.00	6.99	
E	23	Mu	R-Isopropyl	S-Benzyl	Norbornylmethyl	>1000	>1000	>10,000	6.00	6.00	
	24	Mu	R-Isopropyl	S-Benzyl	Cyclopentylmethyl	>1000	>1000	>10,000	6.00	6.00	
F	25	Mu	R-Isopropyl	R-Isopropyl	Benzyl	>1000	>1000	>10,000	6.00	6.00	
	26	Mu	R-Isopropyl	R-Isopropyl	Isobutyl	>1000	>1000	>10,000	6.00	6.00	
	27	Mu	R-Isopropyl	R-Isopropyl	Norbornylmethyl	>1000	>1000	>10,000	6.00	6.00	
	28	Mu	R-Isopropyl	R-Isopropyl	Cyclopentylmethyl	>1000	>1000	>10,000	6.00	6.00	
G	46	Kappa	R-4-Hydroxybenzyl	S-4-Hydroxybenzyl	2,2-Dimethylpropyl	>1000	387	4551	6.00	6.41	
H	54	Kappa	R-n-Butyl	R-4-Hydroxybenzyl	Isopropyl	>1000	102	>10,000	6.00	6.99	
	56	Kappa	R-n-Butyl	R-4-Hydroxybenzyl	Cycloheptyl	>1000	161	>10,000	6.00	6.79	

TPI 762
N-methylated 1,3,4-trisubstituted triamine

TPI 761
N-benzylated 1,3,4-trisubstituted piperazine

A. B. Yongye et al./Bioorg. Med. Chem. 17 (2009) 5583–5597

5585

Table 1 (*continued*)

Set	Molecule	Receptor[a]	R1	R2	R3	μIC_{50} (nM)	κIC_{50} (nM)	δIC_{50} (nM)	pIC_{50} μ	pIC_{50} κ	Scaffold
I	59	Mu	S-4-Hydroxybenzyl	Hydrogen	Cycloheptyl	152	93	>10,000[b]	6.82	7.03	
	60	Mu	S-4-Hydroxybenzyl	Hydrogen	Norbornylmethyl	167	373	1956	6.78	6.43	
J	61	Mu	S-4-Hydroxybenzyl	S-Isopropyl	3-Methylbenzyl	206	1000	>10,000	6.69	6.00	
	64	Mu	S-4-Hydroxybenzyl	S-Isopropyl	Norbornylmethyl	223	374	>10,000	6.65	6.43	
K	66	Mu	R-4-Hydroxybenzyl	Hydrogen	Isopentyl	471	1000	>10,000	6.33	6.00	
	67	Mu	R-4-Hydroxybenzyl	Hydrogen	Cycloheptyl	90	223	>10,000	7.05	6.65	
	68	Mu	R-4-Hydroxybenzyl	Hydrogen	Norbornylmethyl	92	476	>10,000	7.04	6.32	
L	69	Mu	R-4-Hydroxybenzyl	S-Isopropyl	3-Methylbenzyl	>1000[b]	>1000	>10,000	6.00	6.00	
	70	Mu	R-4-Hydroxybenzyl	S-Isopropyl	Isopentyl	>1000	>1000	>10,000	6.00	6.00	
	71	Mu	R-4-Hydroxybenzyl	S-Isopropyl	Cycloheptyl	>1000	>1000	>10,000	6.00	6.00	
	72	Mu	R-4-Hydroxybenzyl	S-Isopropyl	Norbornylmethyl	>1000	>1000	>10,000	6.00	6.00	
M	73	Kappa	S-1-Methylpropyl	R-Isopropyl	2-Cyclohexylethyl	>1000	58	>10,000	6.00	7.24	
	74	Kappa	S-1-Methylpropyl	R-Isopropyl	Adamantylmethyl	>1000	119	>10,000	6.00	6.92	
	75	Kappa	S-1-Methylpropyl	R-Isopropyl	Norbornylmethyl	>1000	1000	>10,000	6.00	6.00	
N	79	Kappa	R-4-Hydroxybenzyl	R-Isopropyl	2-Cyclohexylethyl	920	654	>10,000	6.04	6.18	
	81	Kappa	R-4-Hydroxybenzyl	R-Isopropyl	Norbornylmethyl	336	230	>10,000	6.47	6.64	

TPI 760
N-methylated 1,3,4-trisubstituted piperazine

[a] Receptor for which each compound was predicted active from the screening of the mixtures.

[b] For this work the activity was approximated as IC_{50} = 1000 (μ and κ-receptors) or 10,000 (δ-receptor).

Overall, when R2 was *R*- or *S*-isopropyl, and R1 was *R*-4-hydroxybenzyl five out of six compounds that satisfied these conditions were inactive: **69**, **70**, **71**, **72**, and **79** were inactive, while only **81** was active. Based on these activities, the following trends were observed in the compounds derived from the 760 library: R1 = *S/R*-aromatic, R2 = hydrogen and R3 = aromatic/cyclic would lead to active compounds; less bulky substituents were preferred at R2; if R2 were to constitute bulky groups, an *S*-aromatic group at R1 would increase the probability of producing an active compound.

The following rules emerged from the structure–activity:

Compounds from library 762 (**1–20**)

1. R1 and R2 = aromatic (*S*-4-hydroxybenzyl) = active. Compounds **1–5**.
2. R1 = aromatic (*S*-4-hydroxybenzyl), R2 = acyclic aliphatic (*N*-propyl) = generally more active in the κ-receptor. Compounds **7–10**.
3. R1 = acyclic aliphatic (*N*-propyl), R2 = aromatic (*S*-4-hydroxybenzyl) = generally more active in the μ-receptor. Compounds **11–15**.
4. R1 and R2 = acyclic aliphatic (*N*-propyl) = inactive, except **20** that was active in the κ-receptor.

Compounds from Library 760 (**59–81**)

1. R2 = hydrogen, all (five) of the compounds are active in the μ-receptor regardless of the R1 and R3 substituents: **59**, **60**, **66**, **67** and **68**. All were active in the κ-receptor except **66** that was neither aromatic nor cyclic at R3. Rule: R1 = *S/R*, R2 = hydrogen, R3 = aromatic/cyclic gives active compounds.

2. Unfavorable binding when R2 was bulky. Comparing compounds **60** (R2 = hydrogen) and **64** (*S*-isopropyl): *S*-ispropyl at R2 reduced binding slightly; active, **66** (R2 = hydrogen) and inactive, **70** (R2 = isopropyl); active, **67** (R2 = hydrogen) and inactive, **71** (R2 = isopropyl); active, **68** (R2 = hydrogen) and inactive, **72** (R2 = isopropyl).
3. R2 *S*-stereochemistry and R1 *R*-hydroxybenzyl resulted in poor binders. Compounds **69–72**, and the comparison of sets **61–69** and **64–72**.
4. Aromatic groups were important for binding to the μ-receptor. Compounds **73–75**. When R2 was not hydrogen, and R1 was *S*-1-methylpropyl all (three) are inactive in the μ-receptor. Compounds **73** and **74** are active in the κ-receptor, akin to compound **20** in the 762 library series.
5. When R2 was not hydrogen, and R1 was *S*-4-hydroxybenzyl the compounds were active in the μ-receptor, compounds **61** and **64**. Compound **61** was inactive in the κ-receptor.
6. When R2 was *R/S*-isopropyl, and R1 was *R*-4-hydroxybenzyl five out of six compounds that satisfied these conditions were inactive: **69**, **70**, **71**, **72**, and **79** were inactive, while **81** was active. Therefore, an *R*-4-hydroxybenzyl at R1 and a bulky group at R2 would not be good for generating active compounds.

2.3. Binding mode generated by similarity-based molecular alignment

A popular way for binding mode prediction involves automated docking in which the geometry of the receptor utilized is commonly obtained from either X-ray crystallography or NMR,
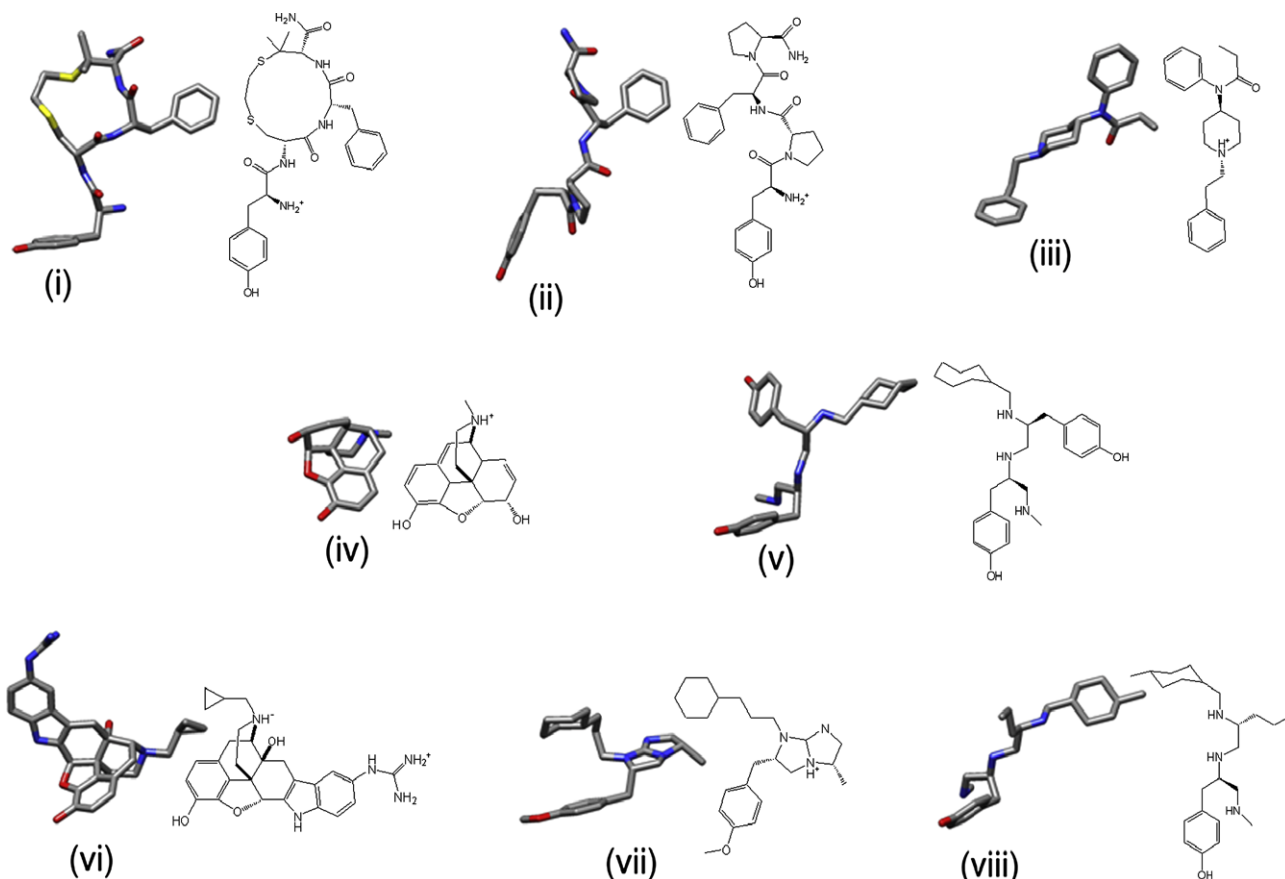

Figure 1. Structures of receptor-selective query molecules employed in the 3D similarity search: (i) JOM6; (ii) morphiceptin; (iii) fentanyl; (iv) morphine; (v) μ-internal query, *iq*(μ); (vi) 5′-guanidinium naltrindole; (vii) bicyclic guanidine; (viii) κ-internal query *iq*(κ).

known as structure-based methods. In the case of GPCRs, several homology models have been developed based on the X-ray structure of rhodopsin.[21] Such homology models have be used for docking studies and virtual screening.[22] On the other hand, ligand-based methods can be employed to predict binding modes or perform virtual screening. In ligand-based approaches, one or more active molecules are used as references to identify structurally similar molecules. The performances of automated docking and shape-matching have been compared.[23]

In this work, the molecules shown in Table 1 were overlaid with four known μ-ligands from the literature namely: *morphine*, *fentanyl*, *JOM6*,[24] and *morphiceptin*. In addition, the compound that showed the best binding affinity to the μ-opioid receptor (compound **1**, Table 1) among the molecules in the dataset was also employed as a query, referred to as the μ-internal query or *iq(μ)*. To explore κ activities, three selective κ-opioid ligands were used as reference molecules: 5′-guanidinium naltrindole, a bicyclic guanidine obtained in our laboratory,[12] as well as the most active κ-ligand (compound **7**, Table 1) among the molecules in the dataset

(called here *iq(κ)*), Figure 1. The conformation and orientation of the queries in the opioid receptors were derived based on the conformation of *JOM6* in the activated binding site of the homology model of the μ-opioid receptor, and were kindly provided by the Mosberg laboratory.[24] The 3D coordinates of fentanyl were provided by the Micovic laboratory, based on their studies of complexes between the μ-opioid receptor and fentanyl analogs.[25] A bottleneck in similarity searching resides in the selection of the conformation(s) of query molecules when no experimentally determined bound conformation is available.[17] In an effort to employ meaningful conformations of the queries (*morphiceptin*, *iq(μ)* and *iq(κ)* in this work) we are developing a methodology that takes into account the biological activity and interactions with the receptor.[26] The resulting geometries are shown in Figure 1.

2.3.1. 3D molecular alignments

Details of the 3D molecular alignments are described in Section 4. Tables 3 and 4 show the similarity values for the best overlay found for each molecule in the database with respect to the differ-

Table 2
Similarity values and statistics of the molecules in the database, using four μ-selective query molecules and the internal query, based on Tanimoto coefficient considering electrostatic potential

Name	*iq(μ)*	JOM6	Morphiceptin	Fentanyl	Morphine	Mean	Min	Max
1	2.00	0.72	0.94	1.24	0.93	1.16	0.72	2.00
2	1.65	0.88	1.22	1.24	0.93	1.18	0.88	1.65
4	1.63	0.94	1.10	1.22	0.82	1.14	0.82	1.63
5	1.75	0.96	1.09	1.13	1.08	1.20	0.96	1.75
6	1.42	0.89	1.10	1.31	0.88	1.12	0.88	1.42
7	1.24	0.90	1.05	1.37	0.92	1.10	0.90	1.37
8	1.37	1.01	1.08	1.19	1.00	1.13	1.00	1.37
9	1.44	1.03	0.98	1.33	0.93	1.14	0.93	1.44
10	1.43	0.84	0.86	1.24	1.11	1.10	0.84	1.43
11	1.63	0.67	0.92	1.12	0.95	1.06	0.67	1.63
12	1.60	0.75	0.89	1.22	0.93	1.08	0.75	1.60
14	1.56	0.93	0.94	1.07	0.91	1.08	0.91	1.56
15	1.45	0.74	0.89	1.20	0.88	1.03	0.74	1.45
16	1.26	0.77	1.05	1.26	0.97	1.06	0.77	1.26
17	1.25	0.79	1.08	1.13	0.77	1.00	0.77	1.25
18	1.20	0.80	0.89	1.17	0.45	0.90	0.45	1.20
19	1.15	0.75	1.12	1.28	0.70	1.00	0.70	1.28
20	1.12	0.77	0.98	1.19	0.81	0.98	0.77	1.19
23	0.99	0.78	1.10	1.33	0.74	0.99	0.74	1.33
24	1.02	0.99	1.16	1.36	0.74	1.05	0.74	1.36
25	1.10	0.83	1.00	1.38	0.78	1.02	0.78	1.38
26	1.08	0.90	1.02	1.26	0.84	1.02	0.84	1.26
27	1.06	0.89	1.05	1.49	0.78	1.05	0.78	1.49
28	0.99	0.89	0.95	1.46	0.81	1.02	0.81	1.46
46	1.05	0.93	0.99	1.17	0.67	0.96	0.67	1.17
54	1.03	1.03	1.04	1.46	0.79	1.07	0.79	1.46
56	0.89	0.97	0.97	1.33	0.71	0.97	0.71	1.33
59	1.33	0.91	1.03	1.34	0.86	1.09	0.86	1.34
60	1.46	0.85	1.17	1.30	0.84	1.12	0.84	1.46
61	1.21	1.07	1.03	1.35	0.81	1.09	0.81	1.35
64	1.24	0.91	1.06	1.59	0.84	1.13	0.84	1.59
66	1.25	0.68	1.00	1.34	1.03	1.06	0.68	1.34
67	1.38	0.77	1.05	1.33	0.89	1.08	0.77	1.38
68	1.33	0.83	1.10	1.41	0.89	1.11	0.83	1.41
69	1.10	1.00	0.91	1.27	0.78	1.01	0.78	1.27
70	1.12	0.95	1.01	1.41	0.91	1.08	0.91	1.41
71	1.08	0.88	1.03	1.33	0.84	1.03	0.84	1.33
72	1.09	1.01	0.96	1.56	0.81	1.09	0.81	1.56
73	1.07	0.90	0.98	1.44	0.85	1.05	0.85	1.44
74	1.04	0.98	1.04	1.33	0.73	1.02	0.73	1.33
75	1.02	0.93	1.14	1.47	0.82	1.08	0.82	1.47
79	1.09	0.94	0.91	1.60	0.87	1.08	0.87	1.60
81	1.12	1.11	0.98	1.57	0.81	1.12	0.81	1.57
Mean	1.26	0.88	1.02	1.32	0.85			
Min	0.89	0.67	0.86	1.07	0.45			
Max	2.00	1.11	1.22	1.60	1.11			

iq(μ) = Internal query molecule.

ent queries. Statistics per query are presented at the bottom of the tables. The *mean* and *maximum* values per molecule are shown as *mean* and *max*, respectively. These *mean* and *max* values are examples of data fusion measurements. The use of these measurements in a single 2D-graph has recently been reported and termed multifusion similarity (MFS) maps.[27] Figure 2A shows the MFS map obtained when all query molecules were used. The *X*-axis represents the *mean* combo score similarity of a given molecule towards all queries, while the *Y*-axis represents the *maximum* combo score similarity of a given molecule to either query. Data points at the top right of the plot (high *average* and high *maximum* similarity) indicate molecules that are more structurally similar to the query set than molecules represented by data points at the lower left of the diagram (low *average* and low *maximum* combo score similarity). Data points depicted in Figure 2 are color coded by either μ or κ IC$_{50}$ values (see Table 1). Selected corresponding compound numbers are indicated in the plot. It was observed that all the μ-active compounds (18 molecules) were grouped at the top of the *Y*-axis (*max*) above a combo score value of 1.3, while eight

Table 3
Similarity values and statistics of the molecules in the database, using to two κ-selective query molecules and the internal query, based on Tanimoto coefficient considering electrostatic potential

Name	$iq(\kappa)$	BCG531	5′-GNTI	Mean	Min	Max
1	1.34	1.31	0.92	1.19	0.92	1.34
2	1.47	1.21	0.98	1.22	0.98	1.47
4	1.43	1.19	1.03	1.21	1.03	1.43
5	1.47	1.14	0.90	1.17	0.90	1.47
6	1.63	1.34	0.81	1.26	0.81	1.63
7	2.00	1.28	0.94	1.41	0.94	2.00
8	1.79	0.97	0.79	1.18	0.79	1.79
9	1.69	1.25	0.94	1.29	0.94	1.69
10	1.70	1.26	0.91	1.29	0.91	1.70
11	1.38	1.37	0.96	1.23	0.96	1.38
12	1.40	1.40	1.18	1.32	1.18	1.40
14	0.99	1.30	1.11	1.14	0.99	1.30
15	1.22	1.35	1.09	1.22	1.09	1.35
16	1.37	1.18	1.17	1.24	1.17	1.37
17	1.44	1.04	1.03	1.17	1.03	1.44
18	1.31	0.97	0.81	1.03	0.81	1.31
19	1.49	1.02	1.12	1.21	1.02	1.49
20	1.50	1.10	1.16	1.25	1.10	1.50
23	0.94	1.12	1.11	1.06	0.94	1.12
24	1.15	0.95	1.19	1.10	0.95	1.19
25	1.04	1.01	1.05	1.03	1.01	1.05
26	1.13	0.92	1.07	1.04	0.92	1.13
27	1.14	0.99	1.11	1.08	0.99	1.14
28	1.03	0.90	1.02	0.98	0.90	1.03
46	1.03	1.14	1.03	1.06	1.03	1.14
54	1.04	1.22	1.01	1.09	1.01	1.22
56	1.04	0.99	0.94	0.99	0.94	1.04
59	1.40	1.34	0.98	1.24	0.98	1.40
60	1.62	1.18	0.95	1.25	0.95	1.62
61	1.18	0.95	1.06	1.06	0.95	1.18
64	1.26	0.93	1.02	1.07	0.93	1.26
66	1.55	1.38	1.03	1.32	1.03	1.55
67	1.53	1.35	0.99	1.29	0.99	1.53
68	1.52	1.32	0.98	1.27	0.98	1.52
69	1.06	1.06	0.99	1.04	0.99	1.06
70	1.19	1.14	1.04	1.12	1.04	1.19
71	1.25	1.03	1.00	1.10	1.00	1.25
72	1.12	1.06	1.01	1.06	1.01	1.12
73	1.13	1.21	1.18	1.18	1.13	1.21
74	1.17	1.09	1.18	1.14	1.09	1.18
75	1.27	1.05	1.17	1.17	1.05	1.27
79	1.27	0.99	0.96	1.07	0.96	1.27
81	1.02	1.03	1.00	1.02	1.00	1.03
Mean	1.32	1.14	1.02			
Min	0.94	0.90	0.79			
Max	2.00	1.40	1.19			

$iq(\kappa)$ = Internal query molecule.

Table 4
Feature frequencies employed in developing the pharmacophore model

Type[a]	Minimum	Maximum	Feature matching tolerance (Å)
A	0	3	2.00
D	0	3	2.00
H	1	2 for μ, 3 for κ	2.50
N	0	0	1.75
P	1	3	1.75
R	1 for μ, 0 for κ	3	2.50

[a] A: hydrogen bond acceptor; D: hydrogen bond donor; H: aliphatic hydrophobic group; N: negatively ionizable group; P: positively ionizable group; R: aromatic hydrophobic group.

inactive molecules were located below a combo score value of 1.3 (Fig. 2A). This value has been reported as a reasonable cut-off when internal queries are included.[26] Under this similarity measure and cut-off these molecules follow the similarity principle which states that structurally similar molecules will have similar biological activity.[18] However, there were 15 additional inactives with a *max* above 1.3. This suggested that additional features that were not captured by the molecular overlay were driving the inactivity of these 15 compounds, or that it was not captured by the molecular overlay obtained with the queries employed. The best differentiation of the data points was obtained when $iq(\mu)$ and *fentanyl* were considered, Figure 2B. With these two queries it was possible to portray a direct comparison (*max* on each axis) in a 2D graph. As expected most of the compounds with similarity values above 1.6 to $iq(\mu)$ were from the 762 library, given that $iq(\mu)$ belonged to this library. Interestingly, four active compounds, **61**, **64**, **66** and **81**, had similarity values less than 1.3 in the $iq(\mu)$-axis, but greater than 1.3 in the *fentanyl*-axis, Figure 2B. Putative binding modes as a result of the comparison of molecule **64** with these two queries are discussed below.

For the κ-receptor, the MFS map displayed properties similar to those of the μ-receptor, Table 3, Figure 2C and D. All the compounds derived from the 762 library were located in the 'active' region of the MFS map (Fig. 2C), while compounds derived from the 761 library (mostly inactives) scored low similarities to the reference molecules. Meanwhile compounds derived from library 760 spanned the similarity cut-off, with five compounds above the combo score value of 1.3 and **11** below. A direct comparison between the *max* similarities with reference to $iq(\kappa)$ and BCG531 is shown in Figure 2D, which is the equivalent to Figure 2B. In contrast to Figure 2B, in this case none of the active molecules had high similarity (above 1.3) to the external query (BCG531) and low similarity (below 1.3) to $iq(\kappa)$. In other words, no additional 'active' molecules were extracted when BCG531 was employed.

Graphical representations of the best overlays within each library obtained from ROCS are illustrated in Figures 3 and 4 for the μ- and κ-query molecules, respectively. The query molecules are shown as licorice, along with their molecular surfaces colored by atom name. The numbers in parentheses correspond to the average similarity values to the queries for the compounds derived from each library. Figure 3 portrays the overlays with $iq(\mu)$ and *fentanyl*. Visual inspection showed that for compounds derived from library 762 the best overlays were obtained with $iq(\mu)$, as expected, whereas for *fentanyl* the best overlays were obtained with compounds derived from library 760. On the other end, compounds derived from library 761 were the most dissimilar to these two queries, but showed a better overlay with *fentanyl* than the compounds derived library 762. Examining the similarity data in Table 2 showed that on average *fentanyl* had higher combo scores with compounds from libraries 761 and 760 confirming the observations in Figure 3. The higher scores for compounds derived from libraries 760 and 761 probably arose from the additional volume
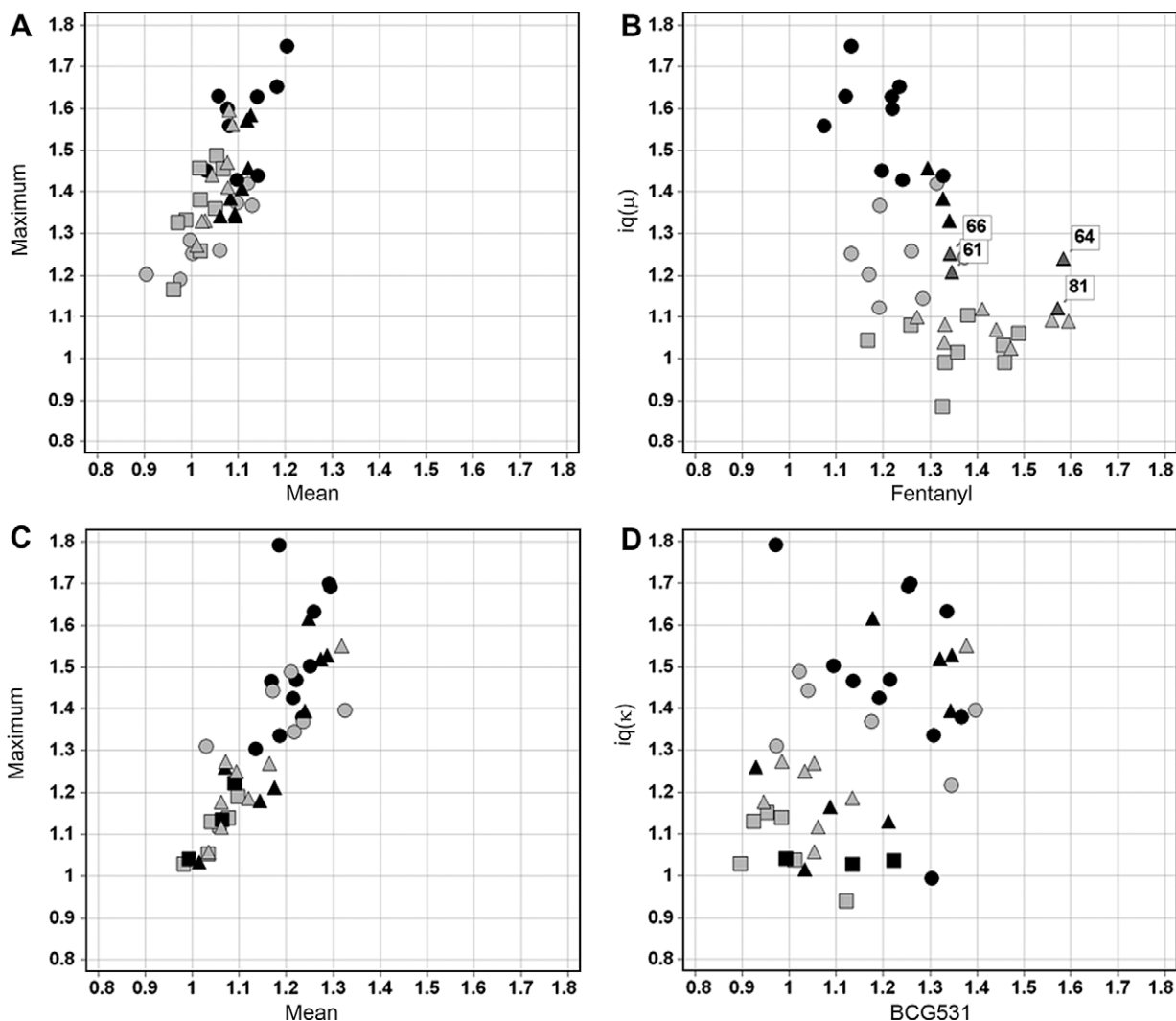
Figure 2. Multi-fusion similarity maps: (A) μ-queries, and (C) κ-queries. B (μ-queries) and D (κ-queries) use only the *max* score towards two query molecules each (B: $iq(\mu)$ = Y-axis; fentanyl = X-axis and D: $iq(\kappa)$ = Y-axis; BCG531 = X-axis). Black: active (<500 nM); gray: inactive ((>500 nM)). The compound classes are: triangles: derived from 760; Squares: derived from 761; Circles: derived from 762.

overlap between the piperazine ring for these compounds (a feature not present in compounds from 762) with the piperidine ring of *fentanyl*.

The overlays with the κ-queries are depicted in Figure 4. As was observed in the case of the μ-queries, library 762 had the highest average similarity with $iq(\kappa)$, followed by library 760 and lastly 761. With the *BCG531* query library 762 had the highest average combo score, followed by library 760 and lastly 761, in qualitative agreement with the affinities of these compounds.

Since the ROCS overlays were produced from the query molecules oriented in the binding pocket of the μ-receptor, it was possible to visualize the ROCS solutions in the receptor's binding site. The overlays obtained here do not assume *a priori* similar orientation of the molecules. The best solution may or may not result from the same orientation with respect to the query molecule. For instance, the overlay of compound **64** with $iq(\mu)$ and *fentanyl* resulted in two different orientations, Figure 5. The overlay with $iq(\mu)$ represented the classic 'message' interaction between opioid ligands and their receptors, involving the tyramine moiety of the ligands.[20] In this orientation the aromatic group of compound **64** interacts with Phe152, Phe237 and Trp293, Figure 5. In addition, the phenolic hydroxyl group forms a hydrogen bond with the Nε atom of His297, while the norbornyl group interacts with other hydrophobic resi-

dues including Phe221 and Trp318. In the overlay with *fentanyl* the norbornyl group primarily makes hydrophobic interactions with Phe152, Phe237, Trp293 and His297. The tyrosine group of the ligand now stacks with Phe221 and Trp318. These alignments may offer different binding modes for these compounds, and bolster the rationale for the frequent practice of utilizing a number of query molecules during 3D similarity searches. A refined search was performed by using an extra parameter 'randomstarts', to further evaluate these two orientations during the similarity search.[28] When this variable was included in our searches with a value of 50, inverted alignments of the R1 and R3 substituents were still obtained. This orientation may be feasible, given that molecular docking studies have been employed to suggest different binding modes for *fentanyl*.[29] The different orientations probably arose from the predominance of hydrophobic groups at the two ends of the compounds. A pharmacophore model was then developed as a complementary ligand-based method, in which the aliphatic hydrophobic sites can easily be distinguished from those that are aromatic, vide infra. Overlays obtained by the comparison of molecules derived from the library 761 resulted in severe steric clashes in the binding pocket. However, they could be accommodated in the binding pocket when the 'message' part of the molecule was not making key contacts with the receptor. Even in some poses
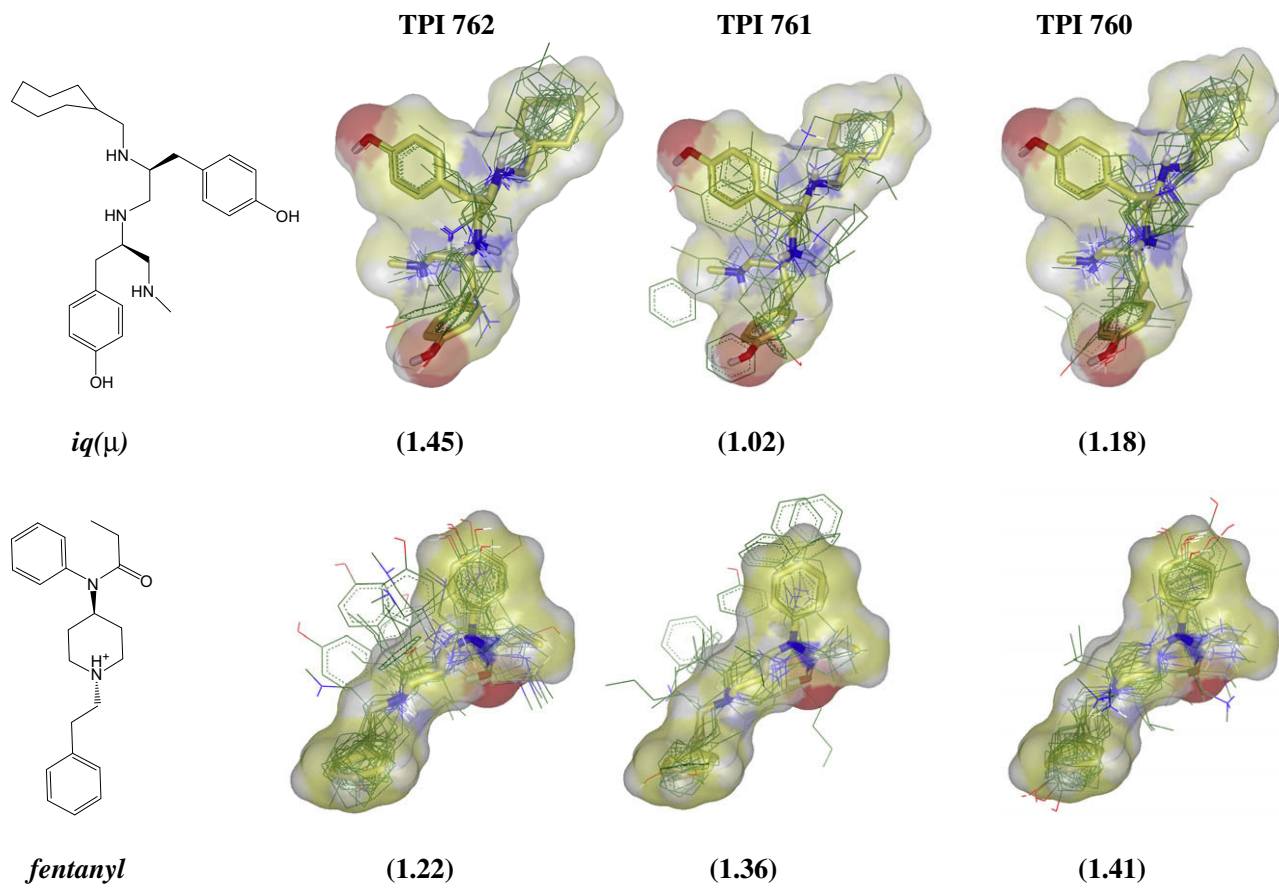
Figure 3. ROCS overlays between two μ-queries and compounds derived from the three libraries in the database. First row: *iq(μ)*; second row: *fentanyl*. The parent libraries are, from left to right: 762, 761 and 760. The average combo score similarities are shown in parentheses.
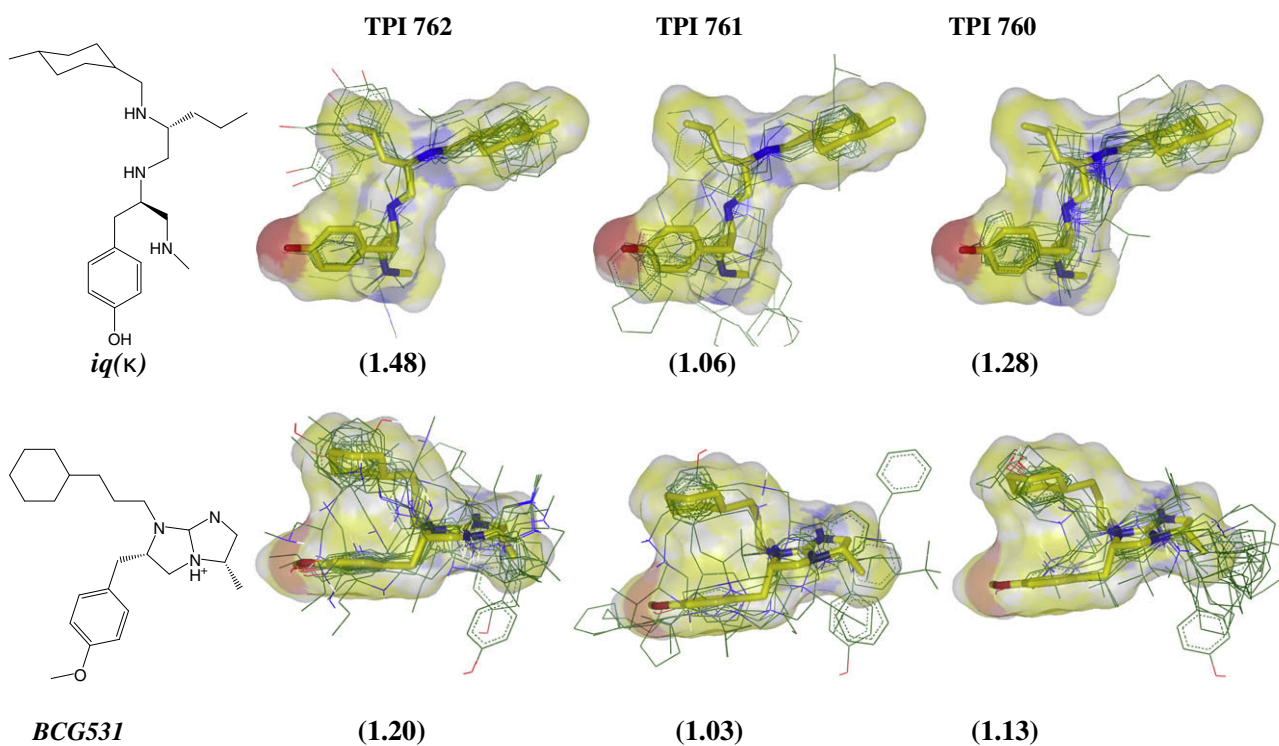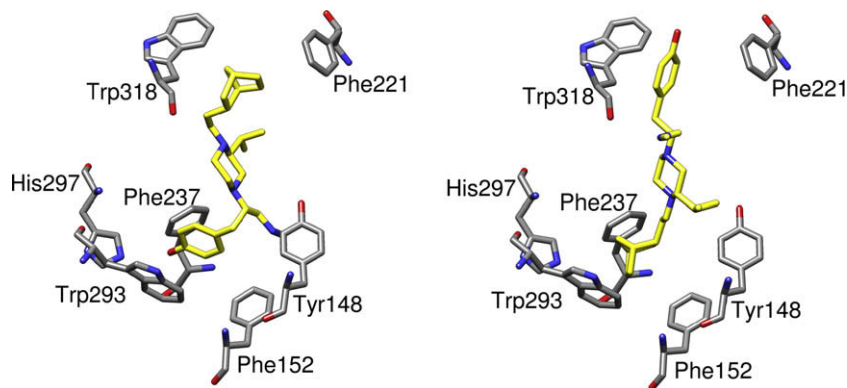

Figure 4. ROCS overlays between three κ-queries and compounds derived from the three libraries in the database. First row: *iq(κ)*; second row: *BCG531*. The parent libraries are, from left to right: 762, 761 and 760. The average combo score similarities are shown in parentheses.

Figure 5. Possible binding interactions of the two orientations of compound **64** with the μ-opioid receptor. The resulting orientations indicate when the compounds were overlaid with *iq(μ)* (left) and *fentanyl* (right).

wherein the 'message' moiety was oriented differently, van der Waals' clashes still occurred. The inability of compounds derived from library 761 to fit into the binding pocket may explain the low binding affinity to either opioid receptor. These findings suggest that the removal of the bulky *N*-benzyl group will alleviate these unfavorable interactions and subsequently improve the activities of these compounds.

2.4. Pharmacophore modeling

2.4.1. Pharmacophore hypotheses

For the μ-receptor, common pharmacophores were determined by employing upper and lower site limits of six and four, respectively, and specifying that pharmacophore features in each valid hypothesis matched all the compounds in the training set. For the κ-receptor six and five sites were used as upper and lower limits, requiring that a hypothesis matched at least 11 of the 13 most active ligands. The feature frequencies employed to generate all the *variants* (particular combination of feature types) are shown in Table 4. The *variants* that met these criteria were scored with the feature matching tolerances also displayed in Table 4. Next, a modified scoring function was employed to score the hypotheses weighting the reference ligand's activity and relative conformational energy by 0.3 and 0.1, respectively. The strategy was to keep the pharmacophore hypotheses with the highest scores that maintained low relative conformational energy of its reference ligand. Hypothesis that survived the scoring are shown in Table 5, along with the corresponding reference compound and relative energies.

2.4.2. Structure–activity relationships based on the alignments with the reference ligands

2.4.2.1. μ Ligands. The alignments with the reference ligand of each hypothesis were employed to rationalize the observed activities of the compounds in the database. In the following paragraphs the alignments with AHPPPR.19 are detailed. In general, the same

conclusions could be derived by the analysis of the alignments with the hypothesis AHPPPR.16. The six-point pharmacophore model for the AHPPPR.19 hypothesis is shown in Figure 6A.

Three different scenarios are exemplified below. The first collects several active molecules correctly aligned with the hypothesis. The second exemplifies molecules with borderline activities (considered inactives) but that contain the site features employed in the model, and the third illustrates when the alignments and relative energies suggest a different binding mode:

(1) During the alignment, compounds **59** (R1 = *S*), **66** (R1 = *R*), **67** (R1= *R*), **60** (R1 = *S*) and **68** (R1 = *R*) matched all six sites very well and all were active, indicating that the R1 stereochemistry was not important when R2 was a hydrogen atom. However, when R2 was *S*-isopropyl the stereochemistry at R1 was important ascertained from the activities of (**61** compared to **69**) and (**64** compared to **72**). A moderate alignment was observed between the reference ligand, **59**, and compounds **61** (active), **69** (inactive) and **72** (inactive), but a good alignment with **64** (active).

(2) When an aromatic group was present at the R1 but not the R2 position, for example, for molecules **6**, **7** and **8** good alignments were displayed with the reference ligand. For these molecules the six sites in the AHPPPR *variant* could be assigned to these compounds, without considering the R2 position. Note, that the activities of two of these compounds are borderline, and the structural differences are minute. For that reason, it is not surprising that the hypotheses can not distinguish these molecules as inactives.

(3) Compounds **11**, **12**, **14** and **15** are all actives but at best only partial alignments were obtained with AHPPPR.19. In particular, the AR sites of these compounds were on R2, and an attempt to overlay these sites resulted in an out-of-plane vertical superposition between their R2 (*S*-4-hydroxybenzyl) substituent and the R1 (*S*-4-hydroxybenzyl) substituent of

Table 5
Variants and pharmacophore hypotheses generated

Receptor	Initial *variants* (# hypotheses generated)	Pharmacophore hypotheses that survived the scoring[a]	Reference compound	Relative energy (kcal/mol)
μ	DHPPPR (5)	AHPPPR.19	59	1.327
		AHPPPR.16	60	1.338
	AHPPPR (5)	AHPPPR.18	60	3.908
		AHPPPR.20	60	8.382
κ	DHPPPR (8)	AHPPPR.9	2	3.046
	AHPPPR (5)			

[a] The feature matching tolerances were relaxed to the (default values + 1.0) A, Table 2. The hypotheses were re-scored using a weight of 0.1 for the relative conformational energy of the reference ligand and weighting the activity of the reference by 0.3. The post-hoc scoring did not alter the ranking.
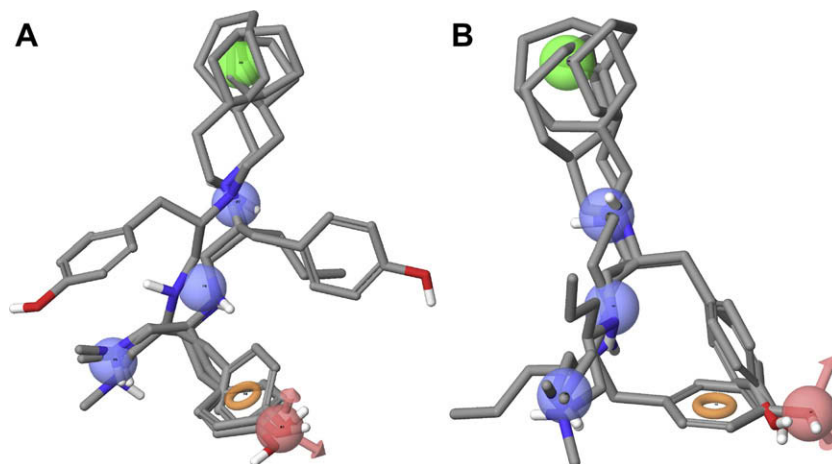
Figure 6. (A) A six site-point pharmacophore model with no site features placed at R2. (B). Overlay of the R2 *S*-4-hydroxybenzyl of compounds **11** and **14**, with R1 *S*-4-hydroxybenzyl of compound **59**. Green: hydrophobic (H); blue: positively ionizable (P); orange: aromatic (R); red: hydrogen bond acceptor (A).

the reference ligand, Figure 6B. This alignment suggested that if these compounds formed complexes with the μ-receptor such that their R2 *S*-4-hydroxybenzyl group occupied the exact position as the R1 *S*-4-hydroxybenzyl group of the reference ligand or the other active compounds, the bound conformers will have very high relative conformational energies that are beyond the 9.55 kcal/mol cut-off specified in the conformational sampling protocol. The relative energies of the superimposed conformers presented here are less than 3.5 kcal/mol: **11** (2.65 kcal/mol), **12** (1.69 kcal/mol), **14** (3.13 kcal/mol) and **15** (3.13 kcal/mol). Thus, it is likely these compounds have a different binding mode.

2.4.2.2. κ ligands. Ligands with aromatic groups at R1 and/or R2 were generally active with the κ-receptor. In most cases, when the R2 hydroxybenzyl group was replaced with an *R*-propyl group, the ligands exhibited about a 10-fold increase in activity, inferred from comparing the activities of compounds **2** with **7** and **5** with **10**. Compounds **1** and **6** were the exceptions in the series in that compound **6** was fourfold less active than compound **1**. Good alignments were obtained for compounds **1 –10,** with fitness above 2.40. Compounds **11**, **12**, **14**, **15**, **54** and **56** showed slightly poorer overlaps due to the alignment of the AR sites on R2 with those of R1 in the reference ligand. Alignments with the inactives (**23–28**) derived from library 761 were generally poor, ranging from 0.09 to 1.27. Despite the presence of an extra *N*-benzyl group in compounds **46**, **54** and **56**, which extended beyond the methyl amine moiety of the reference ligand after the AHPPPR sites were superimposed, the site features overlapped adequately. This was more significant for compound **46** (R1 and R2 = hydroxybenzyl groups), whereby the site features were placed on the aromatic group of R2 resulting in the overlap of the R2 substituent of **46** with the R1 substituent of the reference ligand. The fitness of these compounds were 0.73, 1.44 and 1.68, for **46**, **54** and **59**, respectively, which is in line, qualitatively, with the activities. Particular sets are described below.

(1) An interesting group of active compounds was **20**, **73**, and **74**; they all lacked the AR site features. As a result, their fitness values were all below 1.0; however, their internal alignments were self-consistent. It can be inferred from these activities that the AR sites were not required for these ligands to be active in the κ-receptor, and could represent lead molecules with different pharmacophoric features.

(2) Compounds **59**, **60**, **66** and **68** had good alignments with the reference, Compound **59** (R1 = *S*), **60** (R1 = *S*) and **68** (R1 = *R*) matched all six sites. All these compounds were active, indicating that the R1 stereochemistry was not important when R2 was a hydrogen atom. The outlier in this set was **66** (R1 = *R*), which was inactive in the κ-receptor. It was the only compound within the group, which did not have a cyclic or aromatic substituent at position R3, suggesting that for the κ-receptor the R3 group may be important for this set. A particular case was compound **67** whose best aligned conformation showed a poor overlay at the R3 hydrophobic site feature. In addition, the hydrophobic feature occupied excluded volumes (vide infra) in the hypothesis, signifying the importance of a good alignment protocol when searching for matches in databases with several conformational degrees of freedom.

(3) Compounds **69 –72** with R1 = *R*-hydroxybenzyl and R2 = *S*-isopropyl were inactive. Nonetheless, besides compound **69**, the fitness of the six site features was above 1.5, highlighting how closely related compounds this active and inactive compounds were.

2.4.3. Augmented pharmacophore hypotheses by means of volume spheres and volume cut-off

Aiming to refine the hypotheses, actives and inactives in the training set were aligned, and excluded volume spheres were automatically placed at positions that were occupied only by atoms of the inactive compounds. In this approach, it is postulated that areas of space occupied only by moieties of inactive compounds will result in steric clashes with residues in a receptor. As a final step, a volume cut-off was employed in an attempt to eliminate compounds that did not occupy excluded volumes, but would be considered too small to interact with the receptor. The volume cut-offs ranged from 0% to 100%, Figure 7. The goal was to determine what would be the highest volume overlap that will retain all the actives, but shed a high proportion of the inactives. Figure 7 illustrates that with no restrictions on overlap with the reference ligands about 60% of the molecules in the database are retrieved including all the actives, regardless of the hypothesis for the μ-receptor. However, under the conditions and training set employed for the κ-receptor, when 60% of the entire database was retrieved, only approximately 80% of the active molecules were included. We expected that the curves for the actives to be invariant while those for all the retrieved compounds dropped.
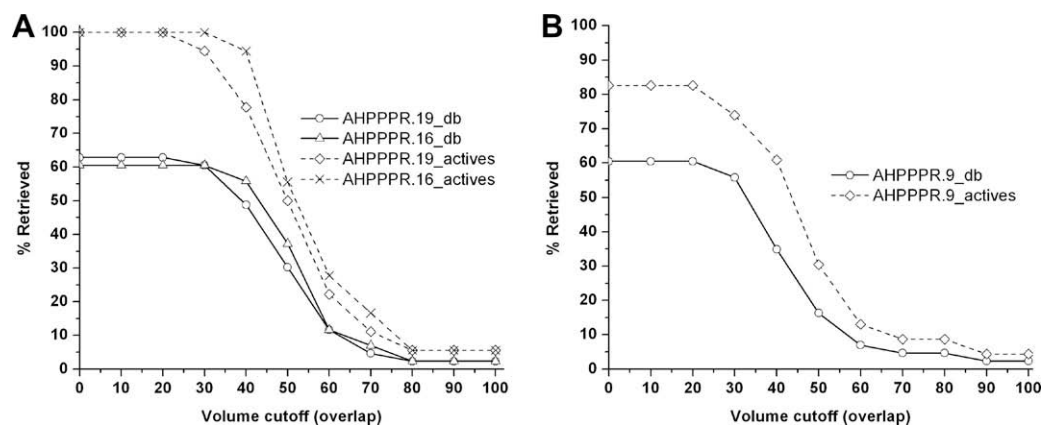
Figure 7. The efficiency of the μ-hypotheses (A) and κ-hypothesis (B) in terms of the percent of all compounds as well as actives retrieved from the database with increasing restrictions on the volume cutoff variable during the database search.

However, in all cases, both sets of curves dropped simultaneously, indicating that employing more restricted models to search the database would result in the loss of active molecules.

In summary, the database search for the μ-activities retrieved **27** and **26** compounds matching six sites for AHPPPR.19 and AHPPPR.16, respectively, containing all the actives (18 compounds). Whereas for the κ-receptor data **26** compounds matched the hypothesis AHPPPR.9, containing 19 out of 23 active compounds, details are described above. In spite of the inherent difficulties faced when dealing with highly flexible and closely related molecules, it was possible to eliminate about 40% of inactive compounds.

It was observed that there were molecules containing the six sites considered here that were inactive. As it has been recognized, the inactivity can be attributed to factors other than the presence or absence of pharmacophoric sites. Conversely a few active molecules were scored unfavorably with the hypotheses, opening the possibility for exploring additional pharmacophore hypotheses.

2.5. Putative interactions in the receptor's binding site

There is a general consensus that the tyramine pharmacophore (phenol and protonated amine) is important for opioid activity acting as a non-selective anchor, 'message', for ligand binding, while the remainder of the ligand, 'address', bestows selectivity to the receptor sub-types. However, there are known examples of opioid receptor active compounds that lack the protonated amine or hydroxyl group.[30] Moreover, Salvinorin A[16] the most potent naturally occurring opioid agonist known, do not contains nitrogen atoms or phenolic groups, indicating the involvement of other mechanisms of opioid receptor activation. Different pharmacophore models have been proposed to rationalize the binding of Salvinorin A to the κ-receptor.[16,30,31] At best, different classes of compounds display different binding features at the same or different binding pockets in a receptor. For instance, the observed activity towards the κ-receptor of compounds **20**, **73** and **74** that lacked the AR sites suggested that these sites may not be required for activity in the κ-receptors, unlike the μ-receptors wherein compounds lacking the AR sites were inactive. This indicated a possible difference in the requirement for ligand binding to these receptors. For compounds **20**, **73** and **74**, it is postulated that these ligands adopt a binding mode in the κ-receptor, which is mediated by hydrophobic interactions and the positively ionizable amine nitrogen atoms, possibly involving extra-cellular loop two (EL2). EL2 is important for κ-activity with dynorphin A (dyn A).[32] This loop partially occupies the entrance to the binding pocket. The 'address' portion of dyn

A bears five basic residues, while the EL2 of the κ-receptor contains seven acidic residues: Glu203, Asp204, Asp 206, Glu209, Asp216, Asp217 and Asp218. In addition there are three acidic residues in the binding pocket: Asp138, Asp223 and Glu297. Therefore, the formation of multiple salt-bridges between the 'address' portion of dyn A and the EL2 of the κ-receptor would be the main driving factor behind the activity of dyn A. In comparison, the EL2 loop of the μ-receptor contains two basic residues: Asp216 and Glu229. There is an additional Glu310 on the EL3 loop of μ-receptor and another Asp147 in the binding pocket. Among the known opioid receptors, the EL2 loop is longest in the κ-receptor, suggesting the binding cavity for this receptor is the smallest. This relatively small cavity may bring the acidic residues in close proximity to interact with the positively ionizable nitrogen atoms for the compounds describe here. The absence of bulky aromatic groups in compounds **20**, **73** and **74** may lead to a greater exposure of the ionizable nitrogen atoms giving rise to the observed activities for these compounds. To investigate further these and other binding features involving these molecules, more refined models will be developed via the utilization of molecular dynamics simulations. Lastly, an estimation of the physico-chemical properties of these compounds computed with QikProp,[33] showed that they are in the range of drug-likeness, selected ADME properties are presented in Supplementary data. Importantly, the most active molecules are predicted not to cross the blood–brain-barrier, which is desirable to prevent the central nervous system-related side effects that usually accompany opioid activation.

2.6. Considerations for virtual screening of combinatorial libraries

The sections above described the application of molecular alignment and pharmacophore development to better understand the structure–activity relationships for the compounds in this study and suggest putative binding modes for these compounds. Such models will be used for the virtual screening of the full parent libraries. In this work, we employed queries from the literature as well as active molecules identified in the library (called here internal queries). It was observed that a ROCS combo score value of 1.3 yielded a differentiation of active from inactive molecules, when the internal queries were employed. The corresponding efficiencies were 86% and 70% for the μ and κ internal queries, respectively. In a recent study Sykes et al. proposed a combo score value of 0.99 as cut-off for the prediction of the active site orientation of a cytochrome P450 2C9 database.[28] By using a similarity cut-off of 0.99 the efficiency of their screening was 89%. When the 0.99 cut-off was utilized with our external queries the calculated efficiencies

were 41% and 54%, for the μ- and κ-queries, respectively. Poor effi-ciencies might be the reflection of significantly different molecular size between the queries and dataset, insufficient conformational sampling in the dataset, poor alignment, or sub-estimation of color matching (matching of heteroatoms), among others. In general terms, although the use of additional parameters for the similarity searches likely increases the computing time, they can be applied to small datasets to alleviate these problems. Some additional con-siderations include the use of Tversky coefficient to take into ac-count the difference in molecular sizes; increment of the number of conformers in the database; and the use of 'randomstarts' to im-prove alignment. In addition, the use of 'fuzzy' molecular represen-tations[34] has been suggested.

In summary, from this work and previous studies,[26] we pro-posed the use of ROCS combo score of 1.3 as cutoff when internal queries are employed in data sets with combinatorial nature. A similarity value of 0.99 has shown good performance as suggested by Sykes et al.[28] for an external query. In any case, the careful selection of the query molecules along with the considerations mentioned above are crucial.

Note that highly dense combinatorial libraries offer a scenario wherein activity cliffs can be identified, and used to develop SAR,[35] whereas the use of external queries might be more appropriate for scaffold hopping. Ultimately, it has been noted that structural simi-larities or dissimilarities between queries and databases do not automatically imply parallel or different biological activity profiles, respectively.[28,36] In this sense, the use of multiple query molecules may alleviate false negatives, and imposing a high threshold for the similarity values may help to avoid false positives.

3. Conclusions

A highly potent and selective triamine to the κ-opioid receptor was identified from a positional scanning combinatorial library. Additionally, non-selective μ–κ binders were obtained. The range of activities in the dataset allowed the development of structure–activity relationships, which are described along with the 3D molecular alignments and pharmacophore models. The low simi-larity values of a subset (compounds from library TPI 761) with the reference compounds, and clashes between its molecular over-laid structures and residues in the receptors pointed to the low activities for compounds in this group. The overlays suggested that the removal of an N-benzyl group may ameliorate the activities of these compounds. The pharmacophore model indicated that the R2 position was not crucial for the activities of the entire dataset; while at least one hydrogen bond acceptor and one aromatic hydrophobic group were required for activity with the μ-receptor. For the κ-receptor two binding modes emerged with one set of compounds employing the hydrogen bond acceptor and aromatic hydrophobic group, while a second set possibly interacted with the receptor via hydrophobic and ionic salt-bridges. These insights will be valuable of the design of new combinatorial libraries target-ing opioid receptors.

4. Methods

4.1. Library synthesis and biological evaluation

The three positional scanning libraries, namely N-methyl-1,3,4-trisubstituted piperazine (TPI 760), N-benzyl-1,3,4-trisubstituted piperazine (TPI 761), and N-methyl triamine (TPI 762) libraries, were generated from resin-bound acylated dipeptides following the strategy outlined in Scheme 1. Reduction of the amides and cleavage of the solid support generated the desired triamines. Treatment of the resin-bound triamines with oxalyldiimidazole and reduction of the oxamide generated, after cleavage of the solid support, the desired trisubstitiuted piperazines.[19,37] Each posi-tional scanning library was made up of three different positions of diversity with one position defined and two mixture positions. The defined R1 position was prepared using 29 amino acids as building blocks, and each mixture having R1 defined contained 1080 compounds. The defined R2 position was prepared using 27 amino acids as building blocks, and each mixture having R2 de-fined contained 1160 compounds. The defined R3 position was
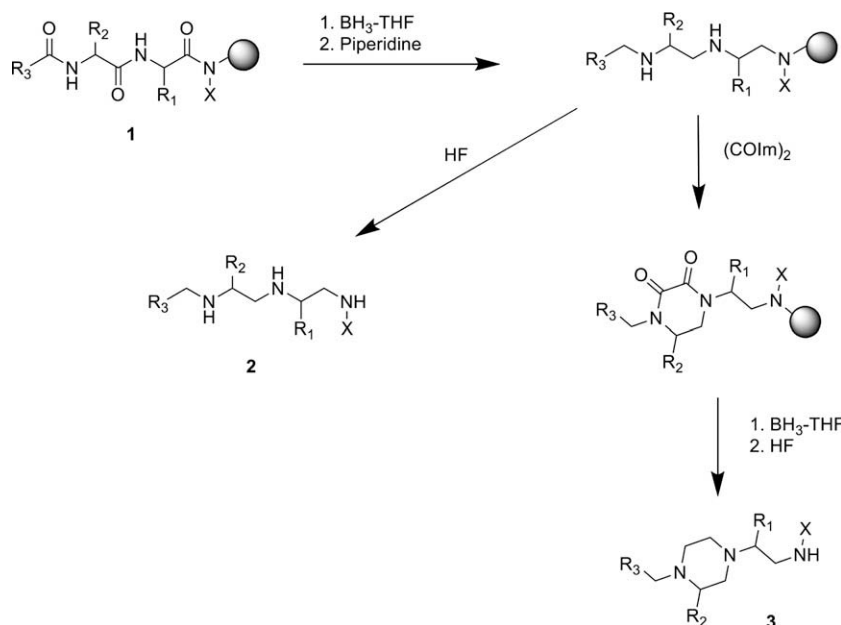
Scheme 1. Solid-phase synthesis of triamines and piperazines from N-acylated dipeptides (**1**). Reduction of the amide groups of the resin-bound N-acylated dipeptide yielded a polyamine. Cleavage of the polyamine with HF yielded the N-methyl triamine (X = methyl). Treatment of the resin-bound polyamine with oxalyldiimidazole yielded the diketopiperazine, and further treatment with diborane in THF followed by HF cleavage yielded the N-methylated and N-benzylated 1,3,4-trisubstituted piperazines (**3**, X = methyl or benzyl).

prepared using 40 carboxylic acids as building blocks, and each mixture having R3 defined contained 783 compounds. Each library has a total of 31320 compounds.

The three positional scanning libraries were screened against the μ, κ, and δ opioid receptors in a competitive receptor binding assay as previously described.[38] Each assay tube contained 0.5 mL of membrane suspension, 3 nM tritiated competitor (mu-DAMGO, kappa-U69,593, or delta-DSLET) and 0.1 mg/mL library mixture (0.008 mg/mL final concentration). Unlabeled receptor-specific ligands (mu-DAMGO, kappa-U50,488, or delta-DSLET) were used as competitors to generate standard curves and determine nonspecific binding for each receptor assay. Mixtures yielding greater than 80% inhibition in each library screening assay were retested in a dose–response assay to determine the most active mixtures at each position of the library. Individual compounds were designed based on combining the functionalities defined in the most active mixtures of each library for each receptor. A set of 84 individual compounds were synthesized and tested against all three receptors and their IC_{50} values were determined.

4.2. Molecular alignment based on 3D similarity

The database consisted of 43 molecules selected from the 84 individual compounds synthesized from TPI 760, 761 and 762, vide supra. The chemical structures of the 43 molecules (Table 1) were built and geometry optimized, using default parameters, the MMFF94x force field and a termination threshold gradient of 0.001 in the Molecular Operating Environment (MOE) software package[39] Next, a multi-conformer library was generated with OMEGA[40] The default parameters were employed while setting the maximum number of conformers per molecule at 5000. The 3D molecular alignments were performed with the Rapid Overlay of Chemical Structures (ROCS) program[41] utilizing the default parameters (exceptions are noted in the text). ROCS maximizes the overlay of the molecular volume of multiple conformers of a given structure in a database with that of a query ligand. The molecular alignments obtained with ROCS were further re-scored with EON,[42] which includes in the scoring scheme a measure of the electrostatic similarity between compounds in the database and the queries.[43]

The queries employed for the alignments were known μ- and κ-selective ligands, Figure 1. The μ-selective ligands were *JOM6*,[24] *morphiceptin*, *fentanyl* and *morphine*, while the κ-selective ligands included *5'-guanidinium naltrindole* (*5'-GNTI*) and a bicyclic guanidine (*BCG531*).[26] In addition to these known queries the most active leads (from the triamine and piperazine libraries) to the μ- and κ-opioid receptors were employed as queries for their respective receptors. These internal queries were referred to as *iq(μ)* and *iq(κ)*. To obtain putative 'bound' conformations of *morphiceptin* and *fentanyl* multiple conformations of each individual molecule were generated utilizing OMEGA,[40] and each conformer was overlaid on the bound conformation of *JOM6* employing ROCS. The conformers with the best ROCS combo score ranking of each molecule were selected as queries. Given the conformationally constrained structures of *morphine* and *5'-GNTI* a ROCS procedure was not necessary. In these instances, their query structures were obtained by superimposing their tyramine moiety with that of *JOM6*. The 'bound' structure of the bicyclic guanidine was in turn generated by overlaying its tyramine moiety with the *JOM6*-superimposed structure of *morphine*. This tyramine fragment, also called the 'message', is known to be one of the key features involved in ligand binding to opioid receptors.[16]

The similarities of the molecules in the database were ranked by their electrostatic Tanimoto values that take into account the chemical nature, molecular shape and electrostatic potentials of the compounds. VIDA[44] and Chimera[45] were used for visualization.

4.3. Pharmacophore modeling

The structures (Table 1) optimized in MOE were converted to the Maestro (.mae) format employing LigPrep.[46] All the molecules in the database were neutral, and were treated as such in LigPrep. The stereochemistry of chiral centers was ascertained from the 3D input structures leading to one stereoisomer per ligand. Next, Confgen[47] was utilized to generate a multi-conformer library in the gas phase. The OPLS_2005 force field was used with a distance-dependent dielectric coupled with an extended interaction cut-off. The optimal minimization protocol was employed with a gradient convergence threshold of 0.001. The input structures were pre-minimized in Confgen for 100 steps, followed by another 100 steps of post-minimization on the generated structures. Ten steps of minimization were allocated for each rotatable bond, while the sampling of the piperazine ring conformations was disallowed. The thorough search mode was employed to generate new conformers. Conformer redundancy was based on comparing only heavy atoms, while an energy window of 40 kJ/mol (9.55 kcal/mol) was selected for saving conformers. At most 5000 conformers were requested per ligand.

4.3.1. Generating hypotheses

The pharmacophore perception was carried out employing Phase version 3.0.[48] The pIC_{50} thresholds for partitioning the active and inactive compounds were set at greater than 6.7 and less than 6.3, respectively. For the μ-receptor this resulted in 9 actives, 25 inactives and 9 uncategorized. The training set of compounds selected for generating the hypotheses consisted of only the active compounds above the 6.7 pIC_{50} threshold. The nine compounds that surpassed the threshold were: **1**, **67**, **68**, **11**, **59**, **60**, **5**, **9** and **14** (see Table 1 and Supplementary data Table S1). Following the same criteria the κ-receptor data resulted in 13 actives, 20 inactives and 10 uncategorized compounds. The 13 compounds selected for the training set are: **7**, **9**, **1**, **10**, **8**, **73**, **59**, **6**, **2**, **20**, **54**, **56** and **5** (Table 1). Note that in order to have a representation of active molecules lacking an aromatic group at positions R1 and R2, compounds **20** and **73** were deliberately included in the training set, whereas molecule **74** was placed in the unclassified category.

Supplementary data

Supplementary data associated with this article can be found, in the online version, at doi:10.1016/j.bmc.2009.06.026.

References and notes

1. Schmauss, C.; Yaksh, T. L. *J. Pharmacol. Exp. Ther.* **1984**, *228*, 1.
2. Cowan, A.; Zhu, X. Z.; Mosberg, H. I.; Omnaas, J. R.; Porreca, F. *J. Pharmacol. Exp. Ther.* **1988**, *246*, 950.
3. Mansour, A.; Khachaturian, H.; Lewis, M. E.; Akil, H.; Watson, S. J. *Trends Neurosci.* **1988**, *11*, 308.
4. May, C. N.; Dashwood, M. R.; Whitehead, C. J.; Mathias, C. J. *Br. J. Pharmacol.* **1989**, *98*, 903.
5. Abdelhamid, E. E.; Sultana, M.; Portoghese, P. S.; Takemori, A. E. *J. Pharmacol. Exp. Ther.* **1991**, *258*, 299.
6. Maldonado, R.; Negus, S.; Koob, G. F. *Neuropharmacology* **1992**, *31*, 1231.

A. B. Yongye et al. / Bioorg. Med. Chem. 17 (2009) 5583–5597

5597

7. Leighton, G. E.; Johnson, M. A.; Meecham, K. G.; Hill, R. G.; Hughes, J. *Br. J. Pharmacol.* **1987**, *92*, 915.
8. Wollemann, M.; Benyhe, S.; Simon, J. *Life Sci.* **1993**, *52*, 599.
9. Leander, J. D. *J. Pharmacol. Exp. Ther.* **1983**, *224*, 89.
10. Lahti, R. A.; Mickelson, M. M.; McCall, J. M.; von Voigtlander, P. F. *Eur. J. Pharmacol.* **1985**, *109*, 281.
11. von Voigtlander, P. F.; Lahti, R. A.; Ludens, J. H. *J. Pharmacol. Exp. Ther.* **1983**, *224*, 7.
12. Houghten, R. A.; Pinilla, C.; Appel, J. R.; Blondelle, s. E.; Dooley, C. T.; Eichler, J.; Nefzi, A.; Ostresh, J. M. *J. Med. Chem.* **1999**, *42*, 3743.
13. Houghten, R. A.; Pinilla, C.; Giulianotti, M. A.; Appel, J. R.; Dooley, C. T.; Nefzi, A.; Ostresh, J. M.; Yu, Y. P.; Maggiora, G. M.; Medina-Franco, J. L.; Brunner, D.; Schneider, J. *J. Comb. Chem.* **2008**, *10*, 3.
14. Pinilla, C.; Appel, J. R.; Borras, E.; Houghten, R. A. *Nat. Med.* **2003**, *9*, 118.
15. Kolinski, M.; Filipek, S. *Open Struct. Biol. J.* **2008**, *2*, 8.
16. Eguchi, M. *Med. Res. Rev.* **2004**, *24*, 182.
17. Eckert, H.; Bajorath, J. *Drug Discovery Today: Technol.* **2007**, *12*, 225.
18. Johnson, M. A.; Maggiora, G. M. *Concepts and Applications of Molecular Similarity*; John Wiley & Sons: New York, 1990.
19. Nefzi, A.; Giulianotti, M. A.; Houghten, R. A. *Tetrahedron* **2000**, *56*, 3319.
20. Kane, B. E.; Svensson, B.; Ferguson, D. M. *AAAPS J.* **2006**, *8*, E126.
21. Palczewski, K.; Kumasaka, T.; Hori, T.; Behnke, C. A.; Motoshima, H.; Fox, B. A.; Le Trong, I.; Teller, D. C.; Okada, T.; Stenkamp, R. E.; Yamamoto, M.; Miyano, M. *Science* **2000**, *289*, 739.
22. Evers, A.; Klebe, G. *Angew. Chem., Int. Ed.* **2004**, *43*, 248.
23. Hawkins, P. C. D.; Skillman, G. A.; Nicholls, A. *J. Med. Chem.* **2007**, *50*, 74.
24. Pogozheva, I. D.; Przydzial, M. J.; Mosberg, H. I. *AAAPS J.* **2005**, *7*, E434.
25. Dosen-Micovic, L.; Ivanovic, M.; Micovic, V. *Bioorg. Med. Chem.* **2006**, *14*, 2887.
26. Martinez-Mayorga, K.; Medina-Franco, J. L.; Giulianotti, M. A.; Pinilla, C.; Dooley, C. T.; Appel, J. R.; Houghten, R. A. *Bioorg. Med. Chem.* **2008**, *16*, 5932.
27. Medina-Franco, J. L.; Maggiora, G. M.; Giulianotti, M. A.; Pinilla, C.; Houghten, R. A. *Chem. Biol. Drug Des.* **2007**, *70*, 393.
28. Sykes, M. J.; McKinnon, R. A.; Miners, J. O. *J. Med. Chem.* **2008**, *51*, 780.
29. Subramanian, G.; Paterlini, M. G.; Portoghese, P. S.; Ferguson, D. M. *J. Med. Chem.* **2000**, *43*, 381.
30. Gentilucci, L.; Squassabia, F.; Artali, R. *Curr. Drug Target* **2007**, *8*, 185.
31. Singh, N.; Cheve, G.; Ferguson, D. M.; McCurdy, C. R. *J. Comput.-Aided Mol. Des.* **2006**, *20*, 471.
32. Wang, J. B.; Johnson, P. S.; Wu, J. M.; Wang, W. F.; Uhl, G. R. *J. Biol. Chem.* **1994**, *269*, 25966.
33. QikProp 3.1, Schrodinger, LLC, New York, NY, 2008.
34. Jenkins, J. L.; Glick, M.; Davies, J. W. *J. Med. Chem.* **2004**, *47*, 6144.
35. Medina-Franco, J. L.; Martinez-Mayorga, K.; Bender, A.; Marín, R. M.; Giulianotti, M. A.; Pinilla, C.; Houghten, R. A. *J. Chem. Inf. Model.* **2009**, *49*, 477.
36. Martin, Y. C.; Kofron, J. L.; Traphagen, L. M. *J. Med. Chem.* **2002**, *45*, 4350.
37. Nefzi, A.; Ostresh, J. M.; Yu, J. P.; Houghten, R. A. *J. Org. Chem.* **2004**, *69*, 3603.
38. Dooley, C. T.; Ny, P.; Bidlack, J. M.; Houghten, R. A. *J. Biol. Chem.* **1998**, *273*, 18848.
39. Molecular Operating Environment (MOE), version 2007, Chemical Computing Group Inc.: Montreal, Quebec, Canada.
40. OMEGA: version 2.2.1 OpenEye Scientific Software: Santa Fe, NM, USA, www.eyesopen.com.
41. ROCS: version 2.3.1 OpenEye Scientific Software: Santa Fe, NM, USA, www.eyesopen.com.
42. EON: version 2.0.1 OpenEye Scientific Software: Santa Fe, NM, USA, www.eyesopen.com.
43. Muchmore, S. W.; Souers, A. J.; Akritopoulou-Zanze, I. *Chem. Biol. Drug Des.* **2006**, *67*, 174.
44. vida: version 2.1.2 OpenEye Scientific Software: Santa Fe, NM, USA, www.eyesopen.com.
45. Pettersen, E. F.; Goddard, T. D.; Huang, C. C.; Couch, G. S.; Greenblatt, D. M.; Meng, E. C.; Ferrin, T. E. *J. Comput. Chem.* **2004**, *25*, 1605.
46. LigPrep 2.2, Schrodinger, LLC, New York, NY, 2008.
47. ConfGen 2.0, Schrodinger, LLC, New York, NY, 2008.
48. Phase 3.0 Schrodinger, LLC, New York, NY, 2008.